The External Electric Field Effects on the Morphology of Phase Separation in a Mixture of Liquid Crystal/Flexible Polymer

Ke Hong, Hongdong Zhang, Yuliang Yang

Department of Macromolecular Science, The Key Lab of Molecular Engineering of Polymers, SMEC, Fudan University, Shanghai 200433, China

Received 2 January 2001; accepted 14 November 2001

ABSTRACT: In this article, the morphologies of phase separation in the mixtures of small molecular liquid crystal and flexible polymers with or without being subjected to the external electric field are preliminarily studied by polarized light microscope. It is found that the characteristic "Swiss cheese" morphology can always be observed for the case of zero field strength. For the case of 1.2 V/μm field strength, it is found that the external electric field make the binodal curves of the phase diagrams shift to higher temperature and the "Swiss cheese" morphology can never be observed. However, the domain growth rate is highly accelerated due to the fact that the electric field oriented liquid crystal phase excludes the polymer coils strongly. © 2002 Wiley Periodicals, Inc. J Appl Polym Sci 86: 250–258, 2002

Key words: morphology; phase separation; liquid crystal; polarizing light microscope; electric field

INTRODUCTION

When a mixture of polymer and liquid crystal (LC) is quenched from a homogeneous state into their thermodynamically inhomogeneous unstable state, the instability of this mixture is driven by the competition between phase separation and nematic ordering.[1–3] The inhomogeneous materials composed of polymer and LC are often called PDLCs (polymer dispersed liquid crystals), which is important for the technological applications in electro-optical devices used for switchable privacy windows, colored film with electrically controllable optical density, temperature sensors, and various other applications.[2,4–14]

Electro-optical performance of PDLC materials depends strongly on the morphology of the phase-separated structure. Therefore, an understanding of processing and morphology in different conditions is crucial for controlling film properties. Although there are many theoretical and experimental studies focused on the morphologies and phase separation kinetics,[15–21] the morphology and phase separation kinetics obtained by imposing external electric or magnetic fields have not been fully considered. In our previous work, the phase diagram of mixture of polymer/LC with an external magnetic field has been theoretically calculated.[22] The theory reveals that the external field promotes the ordering of LC, which strengthens the driving force for the phase separation. Therefore, the binodal curve is shifted to higher temperature and the spinodal curves are substantially changed. However, this thermodynamical equilibrium theory cannot be used to describe the phase separation kinetics and morphologies obtained under such external condition. To the best of our acknowledge, there are no experimental studies on the morphology evolution in a mixture of polymer/LC under an external electric field.

In this work, the experimental results on the phase separation morphology induced by temperature quench in an external electric field are presented and compared to the results without external electric field.

EXPERIMENTAL

In this study, the polymer used is polystyrene (PS) with number-average molecular weight $\overline{M_n}$ = 5.6 $\times$ 10^3 and a polydispersity $\overline{M_w}/\overline{M_n}$ = 1.5, which is determined by gel permeation chromatography (GPC; HP1100, HP Company) in tetrahydrofuran at room temperature. The liquid crystal used in this experiment is a cyano-bipheyl mixture (trade name E7, BDH Chem. Ltd., England). It has a nematic-isotropic transition temperature of T_{NI} = 60°C without external field.

A mixture of E7 and PS in a ratio of 70/30 by weight was dissolved in 1,2-dichloroethane (about 10 wt % E7 and PS) at room temperature. The solution was stirred for 48 h. Then one or two drops of the clear solution

Correspondence to: Yuliang Yang (ylyang@srcap.stc.sh.cm).
Contract grant sponsor: Ministry of S & T.
Contract grant sponsor: NSFC.

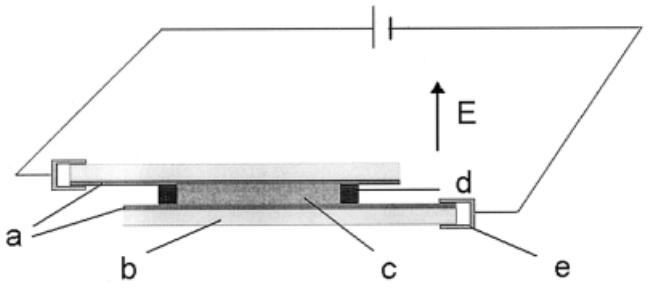

Figure 1 The schematic representation of the experiment: (a) electric layer of conductive glass plate; (b) insulating layer of conductive glass plate; (c) E7/PS film; (d) spacer (20 μm thickness); (e) clasp connected with a direct current circuit. The electric field director is perpendicular to the sample plane.

were sandwiched between two conductive glass plates, separated by spacers of thickness of 20 μm, shown schematically in Figure 1. The samples were placed on a hot ventilation conduction until the most solvent was evaporated and the film specimens became turbid. Afterward the samples were moved into a vacuum oven to evaporate the remaining solvent for a day at 65°C.

After careful elimination of solvent, the samples were prepared in the following way. The specimens were annealed for 1 h at 80°C (well above the phase-separation temperature) to make the specimens homogeneous and to clear up the thermal history. The specimens were then placed on a temperature-controlled stage and investigated by real-time and *in situ* observation under a polarizing light microscope (PLM; orthoplan, Leica Mikrosystems Wetzlar GmbH). The images were video-recorded via a charge coupled devices (CCD) camera and analyzed in a real space. In order to make the observations self-consistent, the viewing areas for the parallel and cross polarizers are kept the same.

For the case with external electric field, the field strength is 24 V (or 1.2 V/μm) of direct current and the electric field direction is perpendicular to the sample plane (Fig.1).

RESULTS AND DISCUSSION

External electric field induced anisotropic phase separation

For the convenience of later discussion, we first schematically show the typical phase diagrams for the LC/polymer mixtures (Fig. 2). We have shown that even for a bulk LC, in the presence of an external field and above the bulk LC transition temperature, the order parameter of LC is still nonzero.[22] We designate this state as paranematic (PN) instead of isotropic when the temperature is higher than LC transition temperature. In Figure 2, it can be seen that, compared to that in a zero field, the paranematic (PN) + homogeneous (H) coexistent phase boundary shifts upward. The isotropic (I) + isotropic (I) coexistent biphasic boundary, which can only be observed when the polymer chain length is high or the isotropic repulsive interaction between LC and polymer is strong, is unaffected by the external field [Fig. 2(b)]. However, due to the increase of the N + PN coexistent biphasic boundary, the PN spinodal region becomes smaller as an imposed external field. It also can be seen from Figure 2 that the nematic (N)-PN phase transition lines shift upward and the N-PN transition temperature increases linearly with increasing LC concentration of φ_L and/or induced an external field.[22,23]

For the sake of comparison, we show the PLM graphs for the case of with and without external electric field in parallel (Figs. 3–7).

For the case without external electric field, the samples annealed at a high temperature were subjected to a temperature drop to various quenching temperatures. The PLM graphs of phase separation morphologies at quenching temperature of 58°C are shown in Figure 3(a). For certain quenching temperatures, a series of PLM graphs were taken for the same area of the same specimen. The corresponding evolution times are indicated on the PLM graphs. The orientations of the polarizer (P) and analyzer (A) are indicated in the figures.

It can be seen from Figure 3(a) that, at quenching temperature of 58°C, only small droplets can be observed in the PLM graph with parallel polarizers at 30 s after quenching. From the evolution of these droplets, it is supposed to be the LC-rich phase. However, nothing can be seen in the PLM graphs with cross polarizers. This reveals that the phase separation is isotropic. When the evolution time reaches 610 s, a polymer-rich continuous phase can be clearly seen. It is remarkable that the nuclei of the LC-rich phase appear at first. The polymer-rich networks are formed surrounding the LC-rich droplets such that the domains exhibit the "Swiss cheese" morphology finally [Fig. 3(a)].[20] This special network-like morphology can be interpreted on the basis of elastic contrast of the components on the phase separation morphology proposed by Tanaka,[24] i.e., LC-rich phase with high elasticity will press the viscous polymer-rich phase into thin layers. The corresponding PLM graphs with cross polarizers show dark images with gray droplets. This reveals that the phase separation is essentially isotropic-isotropic (I-I) phase separation. In addition, the quenching temperature is 58°C, which is very close to the T_{NI} at zero field. Therefore, we can conclude that the phase diagram of the system should be the one shown in Figure 2(b) and the system is located in the I-I region of the phase diagram without external field, which is marked in Figure 2(b).

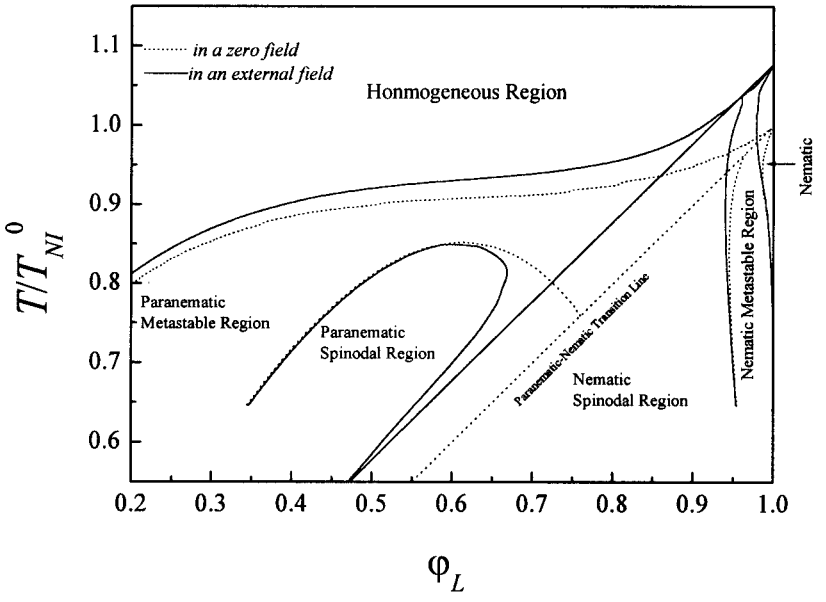

(a)

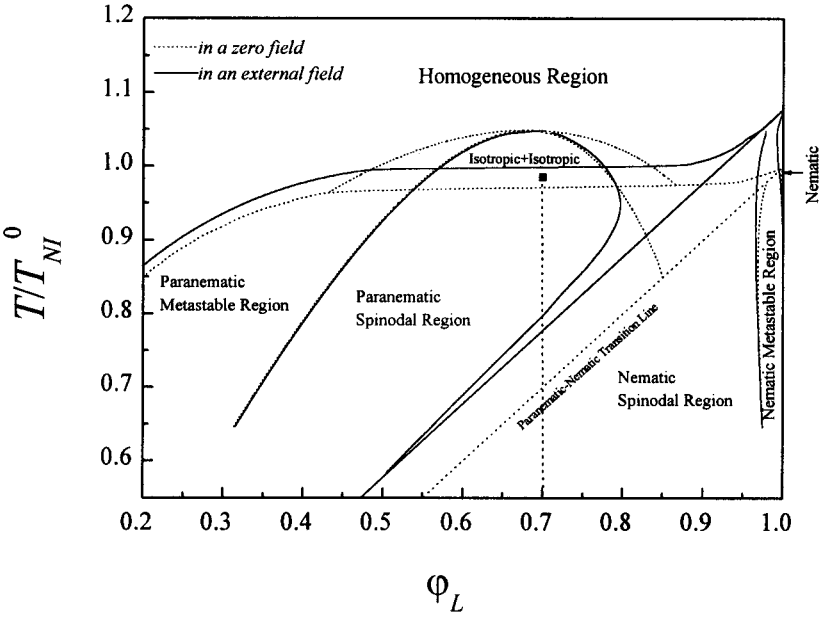

(b)

Figure 2 Phase diagrams and the spinodal lines of polymer–liquid crystal mixtures in a zero field or an external field schematically. T_{NI}^{0} is the transition temperature of the bulk liquid crystal in the absence of an external field, and φ_{L} is a liquid crystal concentration in the polymer-liquid crystal mixtures. (a) T_{NI}^{0} = 308.05 K, chain length x_P = 2.5, Flory–Huggins interaction parameter $\chi_{LP} = 349.71 - 0.0001/T$, and strength of external field is set to $\epsilon = 0.15\varepsilon_{LL}$, where the subscript E_{LL} is the maximum interaction energy between LC molecules. (b) The x_P = 4.5 and the other parameters are the same as in (a).

Now we present the observations on the morphologies of phase separation of the LC/polymer mixture in an external electric field. The PLM graphs for the phase separation subjected to an external electric field at 58°C are shown in Figure 3(b). By comparison of the PLM graphs with parallel and crossed polarizers, it can be observed that the LC-rich domains (appearing as bright droplets under the crossed polarizers) emerge at the evolution time of ~40 s after temperature quench. As the threshold field strength for the alignment of LC is inversely proportional to the radius of LC droplets, i.e., $E_{\mathrm{th}} \propto 1/R$,[25] LC molecules will

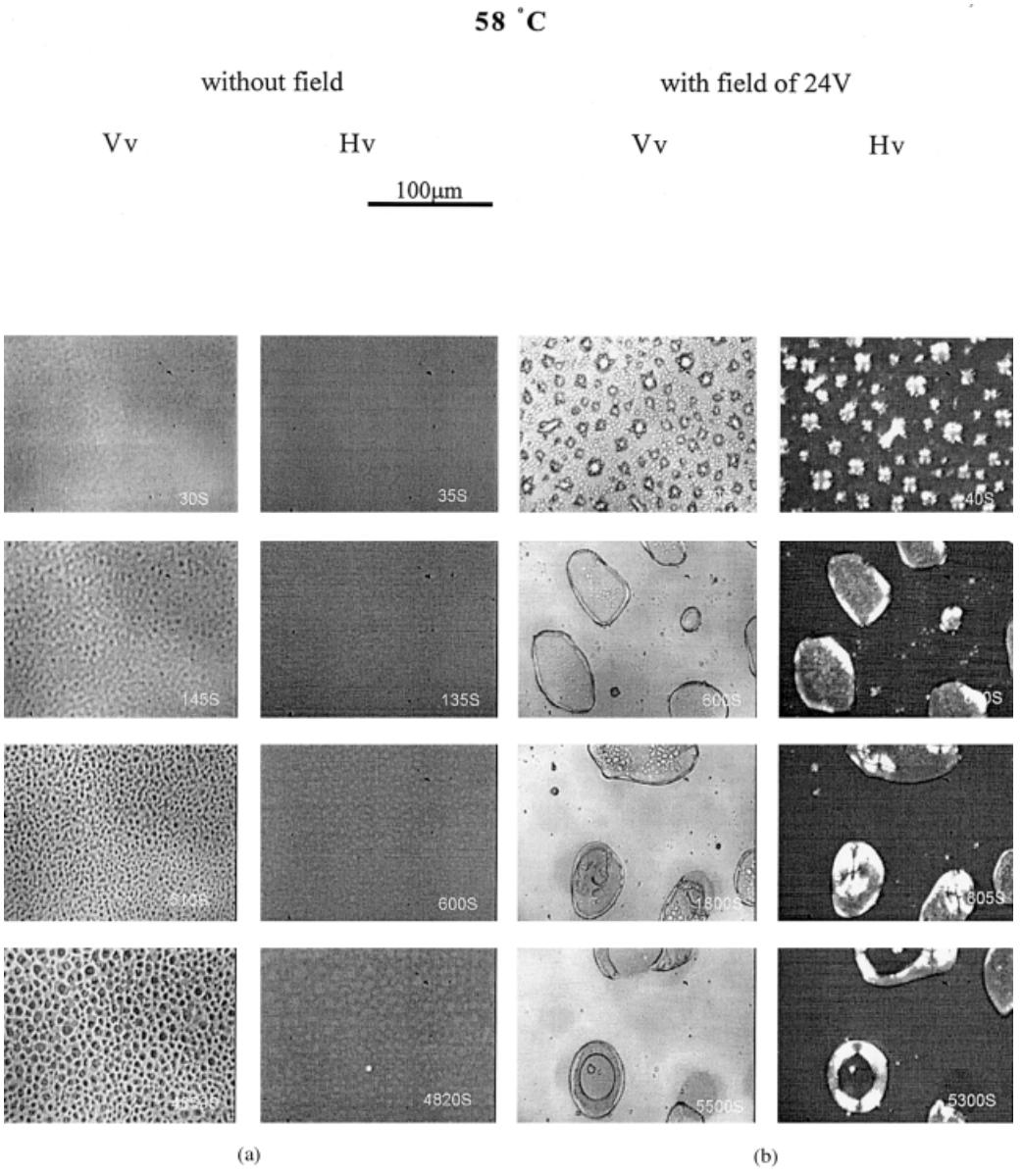

Figure 3 (a) The phase separation is likely an I-I phase separation when the external field is not exerted as the PLM graphs with crossed polarizers are not so bright even at a very late stage (t = 4820 s). (b)When the field strength is 24 V, the LC-rich domains are growing very fast. It is also seen that the director in the middle part of LC droplets is aligned along the electric field. This reveals that the electric field has lifted the binodal curve to the higher temperature. It is also seen that, at the early stage, the LC droplet size is small and the electric field is not strong enough to align the LC molecules. However, after hundreds of seconds, the LC droplets have grown to around 50 μm and the LC molecules in the center of droplets are oriented along the field direction.

align along the field direction easily for the larger droplets. Therefore, the LC molecules will be oriented along the field direction (the normal to the glass plates) when the LC droplets grown to a certain size. The ordered LC will exclude the polymer coils from the nematic phase strongly and thus the driving force for the phase separation is enhanced.[26–28] For this reason, the LC droplets grow much faster than the case of without field. It is known that, for the system of the E7/PS mixture, the director configuration of LC droplets is radial and the LC molecules will be anchored perpendicular to the interface between LC phase and polymer-rich phase.[29] Therefore, the LC molecules in the middle part of droplets are almost oriented completely along the field, which shows the large dark area in the middle of the droplets under cross polarizers, as the threshold field for larger droplets is lower. However, due to the perpendicular surface anchoring for the E7/PS mixture, it shows bright boundaries around the LC droplets. This observation agrees with the typical birefringence patterns for the radial director configuration under the external field.[30]

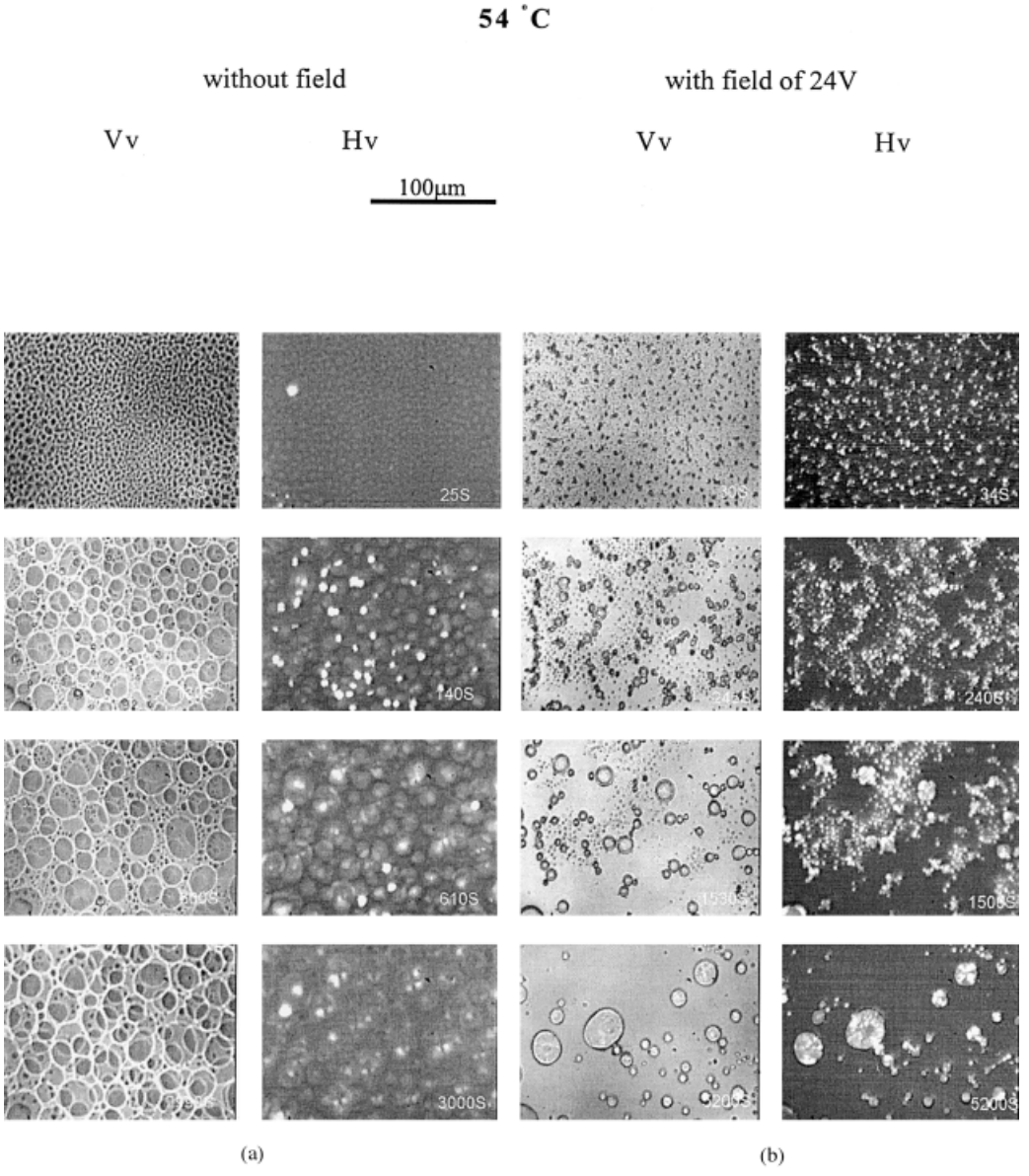

Figure 4 The PLM graphs for the phase separation of LC/polymer mixtures at 54°C (a) in a zero field and (b) in an external electric field of 1.2V/μm.

From the PLM graphs shown in Figures 3–5, we can see that the Swiss cheese morphology could always be observed for the case of zero field. However, it takes shorter time for the appearance of such morphology if the quenching temperatures are low (Figs. 6 and 7). In contrast to that, the "Swiss cheese" morphology can never be observed for all the quenching temperatures when the external electric field is exerted. Unfortunately, at this moment, the mechanism is still not clear.

Quenching depth effect on the kinetics and morphology of phase separation in a zero field

We first discuss the cases without external electric field. Comparing the morphologies of phase separation at the quenching temperatures of 51, 54, and 58°C under zero field, one can find from Figures 3–5 that the Swiss cheese morphologies were formed earlier when the quenching temperature is lower. At temperatures below 54°C, once the LC droplets are born, it grows very fast. At the quenching temperature of 51°C, the diameter of nematic droplets has grown to ~30 μm, which exceeds the thickness of the film, at an evolution time less than 100 s (Figs. 3 and 4).

The morphologies of the films surveyed are not uniform throughout the films, but instead vary with proximity to the film–glass interface. The most general observation is that the drops size is much smaller in the film–glass interface than that in the film midplane. As revealed in the PLM graph with parallel polarizers taken at 130 s in Figure 4(a) and 90 s in

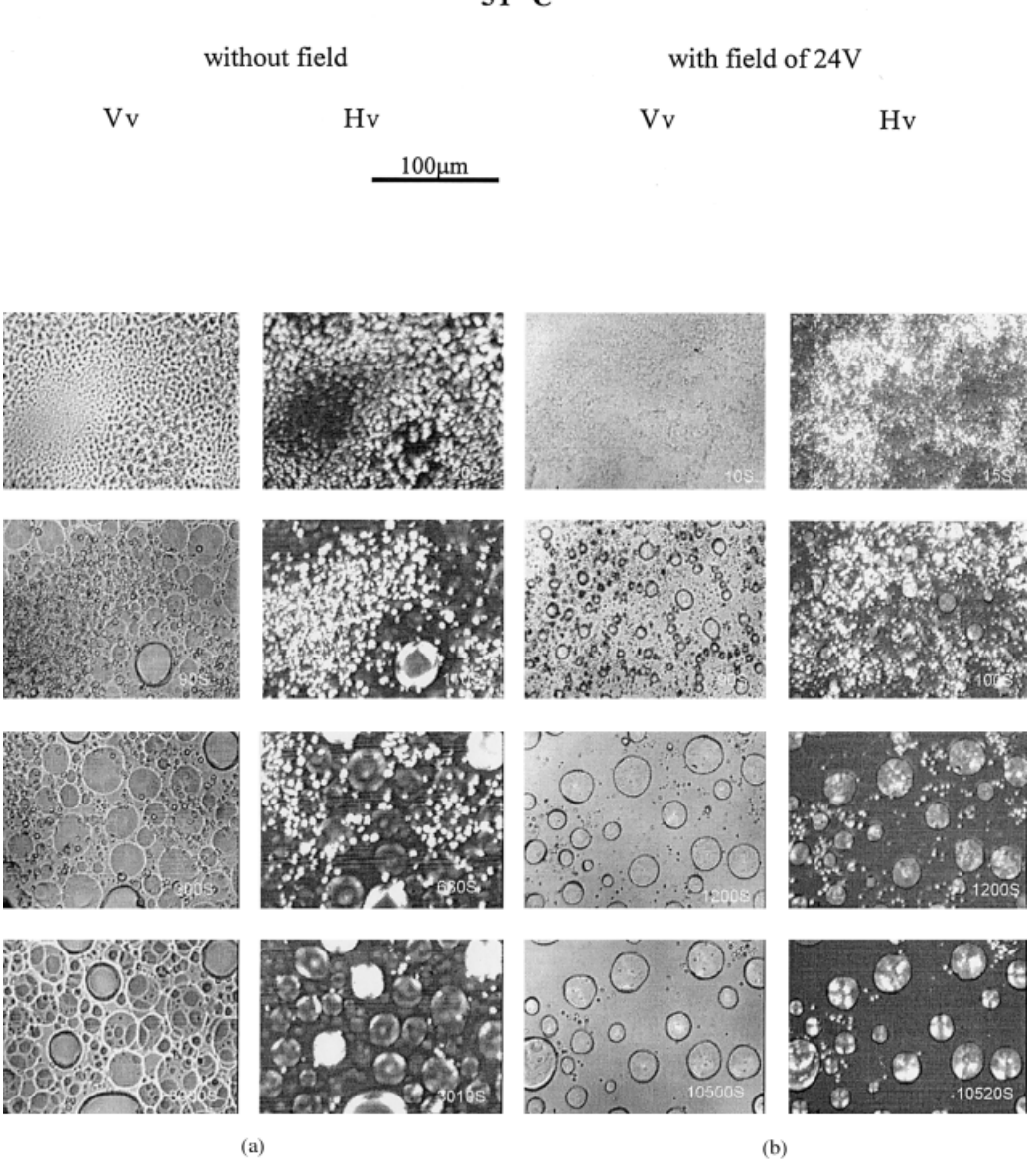

Figure 5 The PLM graphs for the phase separation of LC/polymer mixtures at 51°C (a) in a zero field and (b) in an external electric field of 1.2 V/μm.

Figure 5(a), the small droplets are very near to the film–glass interface, and they are induced by the interfacial effect.[17]

When the temperature is even lower, the kinetics of the phase separation become quite slow due to the low mobility of polymer chains and LC molecules. At the quenching temperature of 40°C, it seems that the Swiss cheese morphology comes out much later [Fig. (6a)]. At the quenching temperature of 30°C, a large number of nondistinctive white droplets can be seen in the PLM graphs in Figure 7(a). This suggests that the nucleation rate of the LC phase becomes much faster but the domain growth rate is largely reduced due to the low mobility of the system at lower temperature. The small droplets grow very slowly due to the domain coarsening is also prohibited. Hence, the dynamical factors are the mainly decisive to the phase-separated structure.

Quenching depth effect on the kinetics and morphology of phase separation subject to an external electric field

For the systems subjected to the external electric field, it is seen that the nematic droplets are dispersed in an isotropic matrix while the Swiss cheese morphology can never be observed [Figs. 3(b)–7(b)].

Due to the fact that the external field shifts the binodal curve to higher temperature, it is clearly seen that the biphasic region is broadened. This results in a

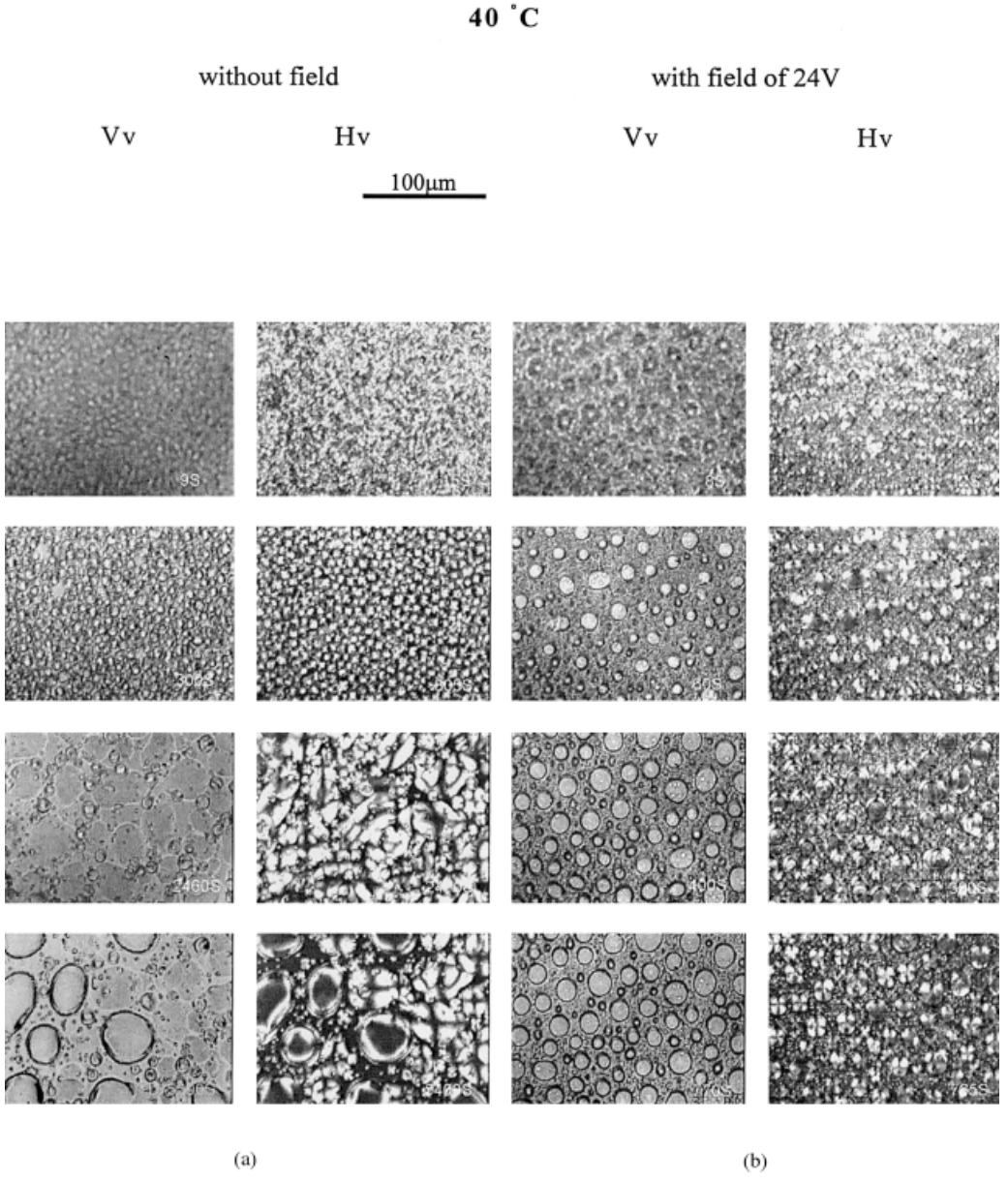

Figure 6 The PLM graphs for the phase separation of LC/polymer mixtures at 40°C (a) in a zero field and (b) in an external electric field of 1.2 V/μm.

larger contrast of refractive indices between the LC-rich phase and polymer-rich phase compared to that in a zero field. This contrast will slightly increase with decrease of temperature. This can be confirmed by careful comparison the PLM graphs with and without external fields shown in Figures 3–7 under parallel and crossed polarizers.

From the PLM graphs shown in Figure 3, it is seen that, at 58°C, the LC-rich droplets are formed at 20s after quenching. Compared to the case of zero field, it is seen that the external electric field not only makes the emerging of the LC droplets much earlier but also enhances the collision and coarsening between LC droplets. However, with decreasing temperature, the collision and coarsening between LC droplets is largely reduced due to the low mobility of polymer chains and LC molecules. This explains that at low quenching temperature, for example, 40 or 30°C, the morphologies of phase separation are almost fixed at less than 800 s after quenching. Therefore, at the late stage, the number of LC droplets generated in an external electric field is much larger than that in a zero field.

If we heat the phase-separated PDLC samples again to get the homogeneous films, it takes a long time to reach the equilibrium state because of no solvent in the films. For reliability, we keep the phase-separated PDLC films at a temperature of 80°C for two weeks. Then we do the same quenching experiments in a zero field or subject to an external electric field. Fortu-

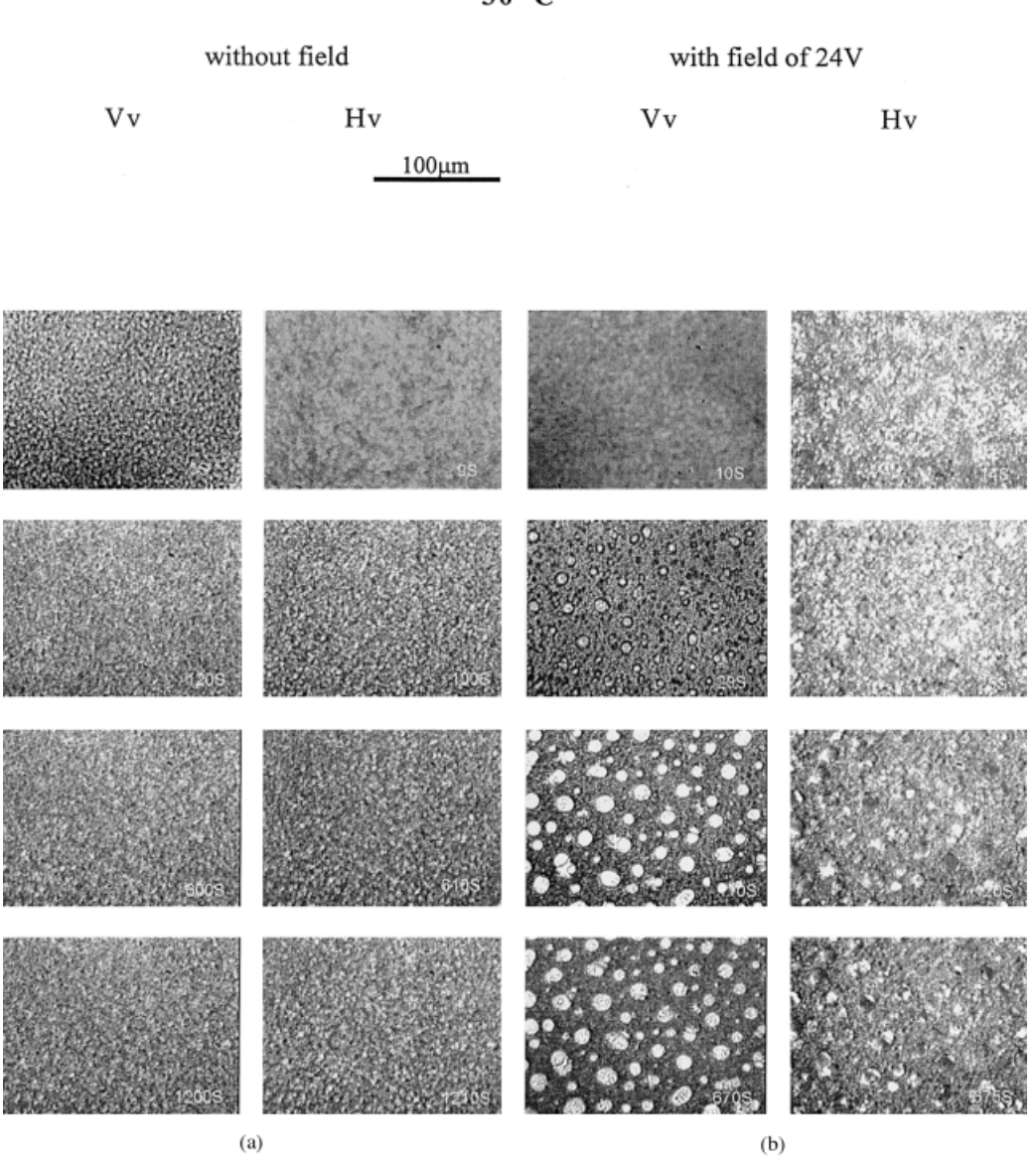

Figure 7 The PLM graphs for the phase separation of LC/polymer mixtures at 30°C (a) in a zero field and (b) in an external electric field of 1.2 V/μm.

nately, the same phenomena can be observed and the morphologies we describe above are not substantially changed.

CONCLUSIONS

In this work, we have shown the preliminary experimental observations on the morphology of phase separation for a mixture of LC/polymer induced by temperature quench in a zero field or an external electric field. Compared to the phase-separated morphology in a zero field, the characteristic of morphology of phase separation in an external field are summarized as follows:

1. It is clearly demonstrated that the external electric field makes the binodal curve of a phase diagram shift upward.
2. For the case of a zero field, a Swiss cheese morphology can always be observed. However, this characteristic morphology can never be observed for the systems subjected to an external field.
3. For the case of shallow quench, the external field accelerates the domain growth rate through the collision and coarsening. However, for the case of deep quench (lower temperature), the rate of collision and coarsening between the LC droplets is largely reduced. Due to

this reason, at the late stage of phase separation, the number of LC droplets is larger and the LC droplet size is smaller compared to the case of a zero field.

We must mention that the results reported here are very preliminary. For many processes, the mechanism is unclear and it deserves further investigations.

This work was subsidized by the Special Funds for Major State Basic Research Projects, Ministry of S & T. Partial financial support from the key project of NSFC, Shanghai Research and Development Center for Polymeric Materials, are also acknowledged.

References

1. Liu, A. J.; Fredrickson, G. H. Macromolecules 1992, 25, 5551.
2. Lin, Z.; Zhang, H.; Yang, Y. Macromol Theory Simul 1997, 6, 1153.
3. Lapena, A. M.; Glotzer, S. C.; Langer, S. A.; Liu, A. J. Phys Rev E 1999, 60, R29.
4. Kajiyama, T.; Nagata, Y.; Maemura, E.; Takayanagi, M. Chem Lett 1979, 679.
5. Graighead, H. G.; Cheng, J.; Hackwood, S. Appl Phys Lett 1982, 40, 22.
6. Doane, J. W.; Vaz, N. A.; Wu, B.-G.; Zumer, S. Appl Phys Lett 1986, 48, 269.
7. West, J. L. Mol Cryst Liq Cryst Inc Nonli Opt 1988, 157, 427.
8. Chidichimo, G.; Arabia, G.; Golemme, A.; Doane, J. W. Liquid Crystals 1989, 5, 1443.
9. Kim, J. Y.; Cho, C. H.; Palffy-Muhoray, P.; Mustafa, M.;. Kyu, T. Phys Rev Lett 1993, 71, 2232.
10. Pan, Y.; Yang, Y. Chem J Chinese Universities [in Chinese] 1994, 15, 1868.
11. Vaz, N. A.; Smith, G. W.; Montgomery, G. P., Jr. Liquid Crystals 1987, 146, 1.
12. Drzaic, P. S. J Appl Phys 1986, 60, 2142.
13. Montgomery, G. P., Jr.; Vaz, N. A. Appl Opt 1987, 26, 738.
14. Kitzerow, H.-S. Liquid Crystals 1994, 16, 1.
15. Parmar, D. S.; Singh, J. J. Liquid Crystals 1993, 14, 361.
16. Nakai, A.; Shiwaku, T.; Wang, W.; Hasegawa, H.; Hashimoto, T. Macromolecules 1996, 29, 5990.
17. Amundson, K.; Blaaderen, A. V.; Wiltzius, P. Phys Rev E 1997, 55, 1646.
18. Lin, Z.; Zhang, H.; Yang, Y. Macromol Chem Phys 1999, 200, 943.
19. Elias, F.; Clarke, S. M.; Peck, R.; Terentjev, E. M. Macromolecules 2000, 33, 2060.
20. Motoyama, M.; Nakazawa, H.; Ohta, T. ; Fujisawa, T.; Nakada, H.; Hayashi, M.; Aizawa, M. Comput Theor Polym Sci 2000, 10, 287.
21. Nwabunma, D.; Chiu, H.; Kyu, T. Macromolecules 2000, 33, 1416.
22. Lin, Z.; Zhang, H.; Yang, Y. Phys Rev E 1998, 58, 5867.
23. Wojtowitz, P. J.; Sheng, P. Phys Lett 1974, 48A, 253.
24. Tanaka, H. J. Phys Condens Matter 2000,12, R207, and references therein.
25. Wu, B. G.; Erdmann J. H.; Doane, J. W. Liquid Crystals 1989, 5, 1453.
26. Yang, Y.; Lu, J.; Zhang, H.; Yu, T. Polym J 1994, 26, 880.
27. Zhang, H.; Li, F.; Yang, Y. Sci In China (series B) 1995, 38, 412.
28. Zhang, H.; Lin, Z.; Yan, D.; Yang, Y. Sci In China (series B) 1997, 40, 128.
29. Ding, J.; Yang, Y. Jpn J Appl Phys 1992, 31, 2837.
30. Ding, J.; Zhang, H.; Lu , J.; Yang, Y. Jpn J Appl Phys 1995, 34, 1928.